

**21st International Conference on  
Harmonisation within Atmospheric Dispersion Modelling for Regulatory Purposes  
27-30 September 2022, Aveiro, Portugal**

---

**POPULATION DYNAMICS AND ITS CONSEQUENCES ON HEALTH RISK MODELING  
FOLLOWING INHALATION EXPOSURE**

*Oscar Björnham<sup>1</sup>, Daniel Elfverson<sup>1</sup> and Leif Persson<sup>1</sup>*

<sup>1</sup>Swedish Defence Research Agency, Umeå, Sweden

**Abstract:**

A crucial part of risk assessment following airborne spread of toxic chemicals is the translation from concentration field to injury probabilities. The impact of population movement remains an understudied and poorly understood factor in such an enterprise. A basic level initiative to target this knowledge gap, with emphasis on a mathematical method to calculate exposure probability distributions, is presented here. Finally, qualitative results from an investigation are presented, which reveal phenomena that are present but hidden in consequence analyses when population movement is ignored.

**Keywords:** *Toxicology, Dynamic population, Health risk, Exposure modeling*

**INTRODUCTION**

The most common method for estimating health risks following an airborne release of toxic chemicals is to apply tabulated values from exposure guidelines, such as AEGL or TEEL amongst many others. These tables present concentration limits for a certain set of chosen exposure times and are compiled by experts using primarily data from animal testing. Even though the tables are very useful, they are burdened by important simplifications that need to be addressed for improved health risk estimations. One evident limitation is that the guidelines are restricted to constant concentration levels, which exclusively is the case in controlled laboratory experiments. For any real life exposure, concentration varies significantly and it is therefore advisable to enhance the exposure modeling to include temporal variance. Improvement may be found by using the well-known probit model, which allows for time variance by its more general construction. Temporal variability of the exposure depends on the dynamics of both the plume itself and the motion of the population. Much effort is today focused on atmospheric dispersion modeling which improves our understanding of the plume dynamics, while modeling of the movement of the population has largely been overlooked and its impact remains to a high degree unresolved.

The intuitive Haber's rule,  $k_{s,e}=cT$ , to describe which exposure time,  $T$ , and concentrations,  $c$ , that are required to obtain a certain medical end point  $e$  for the substance  $s$ , has frequently been used in toxicological studies and risk estimations, as discussed by Miller et al. (Miller et al., 2000). Already in the 1930s, Bliss found that Haber's rule did not fit his experimental data with insecticides, and proposed a toxic load approach (Bliss, 1940). Toxic load,  $T_L$ , is a generalization of Haber's rule by introducing the exponent  $n$  over the concentration, which leads to the toxic load expression  $T_L=c^nT$ . Over the years, many more studies have contradicted Haber's rule and indicated that toxic load provides better agreement to experimental data (Atherley, 1985; Bunce & Remillard, 2003; Gardner et al., 1979; Miller et al., 2000; Ten Berge et al., 1986). Indeed, Haber's rule is only one specific case of the toxic load formulation with  $n=1$ . Probit analysis, i.e. regression using binomial response variables, was suggested by Bliss in 1934 (Bliss, 1934) and has become a popular method. Finney continued on Bliss analysis and established the probit analyses rigorously (Finney & Tattersfield, 1952). Toxicological parameters are typically calculated from controlled conditions where concentrations are held constant. This method allows for characterization of parameters of different substances, which can successfully be applied in risk area estimations. However, in a real-life situation, concentration varies and the expression  $c^nT$  is only applicable for time independent concentrations. Czech et al. discusses different methods to calculate toxic load from time variant concentration field (Czech et al., 2011). The integrated concentration toxic load model

$$T_L = \int_0^T c^n(t) dt \quad (1)$$

is clearly the most consistent method given access to the time-dependent concentration. Equipped with models able to handle nonlinear toxicology and time variant concentration field, we now approach the difficult subject of population dynamics. This is an often-overlooked or ignored aspect in consequence analysis. Indeed, the population is often treated as static (Namboothiri & Soman, 2018; Pontiggia et al., 2010). In contrast, a dynamic population is applied in some hypothetical case studies that thereby catch the combination of concentration plume and a moving population (Georgiadou et al., 2007; Lovreglio et al., 2016; Mocellin & Vianello, 2022; Wang et al., 2020).

To our knowledge, no thorough study has been conducted on the topic of population dynamics coupled to inhalation toxicology. Our ambition is to improve consequence analyses by unraveling the main properties of the interaction between a toxic plume and population dynamics. The initial approach is to identify and investigate the most fundamental and relevant features derived from population dynamics within the framework of probit analysis. To do so, we apply an integrated toxic load model on a population that are allowed to move within a domain containing a concentration field. A static population is considered a special case where the movement speed is reduced to zero. The population is assumed to be unaware of the exposure and do therefore not react in any way to the concentration field. The population dynamics is modeled as a Wiener process using the Itô diffusion framework on a 2D domain without obstacles. This is not a realistic movement of a population but it provides distinct mathematical properties that allow for a wider generalization than a specific case setup would. Even under this simplification, it is reasonable to expect that interesting features can be identified. Provided by knowledge from such a study, realism may later be improved to approach a real-life situation.

In this paper, the emphasis is particularly placed on the methodology to calculate the exposure distributions. Itô diffusion show great compatibility with the Feynman-Kac formula that enables, in a beautiful way, the problem to be cast in the form of partial differential equations (PDE). This transformation allows us to bypass time-consuming Monte Carlo simulations and directly acquire the probability distribution of the exposure with high accuracy and precision by solving the deterministic PDE.

## THEORY

Individuals of the population are modelled to follow random paths  $X(t)$  modelled by Itô diffusions, moving in a given concentration field  $c(t, x)$ . As a consequence of the concentration field and the random path, an individual will be exposed to a random *logarithmic toxic load*, which is referred to as the *exposure*,

$$\Theta = \log \int_0^T c(t, X(t))^n dt \quad (2)$$

during the time interval  $[0, T]$ . A quantal toxicological response (e.g., *light injury*, or *death*) is supposed to occur in an individual if  $\alpha + \beta\Theta$  exceeds an individual *random tolerance*  $\Psi$  (Ashford & Sowden, 1970) which is supposed to be a standard normal random variable. Here  $\alpha$  and  $\beta$  are real numbers, the *probit parameters* for the quantal response in question. At the population level, the probability for the quantal response, referred to as *population injury*, is

$$Q_t = P(\alpha + \beta\Theta \geq \Psi) = \int_{-\infty}^{\infty} P(\alpha + \beta\Theta \geq \Psi | \Psi = \psi) P(\Psi = \psi) d\psi = \int_{-\infty}^{\infty} S_{\Theta} \left( \frac{\psi - \alpha}{\beta} \right) \frac{e^{-\psi^2/2}}{\sqrt{2\pi}} d\psi \quad (3)$$

where  $S_{\Theta} = 1 - F_{\Theta}$  denotes the survival function of  $\Theta$  and  $F_{\Theta}$  is the cumulative distribution function (CDF). The population CDF is obtained by the law of total probability

$$F_{\Theta}(\theta) = \iint F_{\Theta|X(0)}(\theta | x) p(x) dx \quad (4)$$

where  $F_{\Theta|X(0)}(\theta | x) = P(\Theta \leq \theta | X(0) = x)$  is a conditional CDF and  $p(x)$  is the population probability density at  $t = 0$ . The conditional CDF can be obtained from the conditional *moment generating function* (MGF) of  $d = \exp(\Theta)$ , defined by

$$M_{d|X(0)}(t | x) = E[\exp(td) | X(0) = x], \quad t < 0 \quad (5)$$

by deconvolution according to Rossberg (Rossberg, 2008)

$$K * F_{\Theta|X(0)}(y | x) = M_{d|X(0)}(-\exp(-y) | x) \quad (6)$$

Here the convolution kernel is given by

$$K(y) = \exp(-y - \exp(-y)) \quad (7)$$

By the Feynman-Kac formula (Milstein & Tretyakov, 2004)

$$M_{dX(0)}(-\omega | x) = u_\omega(0, x) \quad (8)$$

where  $\omega > 0$  and  $u_\omega(s, x)$  is solution to the terminal value problem

$$\begin{aligned} \partial_s u_\omega(s, x) + L^0 u_\omega(s, x) - \omega c^n(s, x) &= 0, \quad 0 \leq s < T, x \in \mathbb{R}^2 \\ u_\omega(T, x) &= 1, \quad x \in \mathbb{R}^2 \end{aligned} \quad (9)$$

Here

$$L^0 = \sum_{i=1}^2 b_i(s, x) \partial_{x_i} + \frac{1}{2} \sum_{i,j=1}^2 \sigma_{ik}(s, x) \sigma_{jk}(s, x) \partial_{x_i x_j}^2 \quad (10)$$

is the generator of the Itô diffusion

$$dX_i(t) = b_i(t, X(t))dt + \sum_{k=1}^2 \sigma_{ik}(t, X(t))dW_k(t), \quad i = 1, 2 \quad (11)$$

defining the random trajectories of the population. In the method above,  $\mathbb{R}^2$  can be replaced by a bounded domain  $\Omega$ , provided that  $T$  is replaced by  $T \wedge \tau$ , where  $\tau$  is the first exit time of the Itô diffusion, the boundary condition

$$u_\omega(s, x) = 1, \quad 0 \leq s \leq T, x \in \partial\Omega \quad (12)$$

is added in (9), and absorbing boundary conditions are applied in (11), i.e., the right hand side of (11) is multiplied by  $1_{\{\tau > t\}}$ .

## NUMERICAL SOLUTION

To numerically solve the deconvolution equation, eq. (6), to obtain the conditional CDF needed to compute the quantal response, it is reformulated as a minimization problem subject to some extra constraints. It has proven beneficial set up the problem using the PDF instead of the CDF, which is defined by the linear transform

$$L(f_{\Theta|X(0)}(y | x)) = \int_{-\infty}^{\theta} f_{\Theta|X(0)}(y | x) dy = F_{\Theta|X(0)}(y | x) \quad (13)$$

The proposed minimization problem reads:

$$\begin{aligned} \min_{f_{\Theta|X(0)}} & \| K * L(f_{\Theta|X(0)}(y | x)) - M_{d|X(0)}(-\exp(-y) | x) \|^2 + \lambda \| \nabla f_{\Theta|X(0)}(y | x) \|^2 \\ \text{subject to } & f_{\Theta|X(0)}(y | x) \geq 0 \text{ for all } y \in \mathbb{R} \\ & \int_{-\infty}^{\infty} f_{\Theta|X(0)}(y | x) dy = 1 \end{aligned} \quad (14)$$

where the first term is convolution equation and the second term is a penalty which stabilizes the problem by adding additional smoothness, given some penalty parameter  $\lambda$ . The constraints on the PDF directly translates to correct constraints on the CDF, i.e., monotonicity and boundedness in  $[0,1]$ . With a slight abuse of notation the discrete version of equation (14) reads:

$$\begin{aligned} \min_{\mathbf{f}} & \| \mathbf{K}(\mathbf{L}\mathbf{f}) - \mathbf{M} \|^2 + \lambda \| \nabla \mathbf{f} \|^2 \\ \text{subject to } & \mathbf{f}_i \geq 0 \text{ for all } i = 1, \dots, N \\ & \sum_{i=1}^N \mathbf{f}_i = 1 \end{aligned} \quad (15)$$

where  $\mathbf{f}$  is a pointwise approximation of the PDE,  $\mathbf{K}_{j,k} = K(y_j - z_k)(z_{k+1} - z_{k-1})/2$ ,  $\mathbf{M}_j = M_{d|X(0)}(-\exp(-y_j) | x)$ , and  $\mathbf{L}$  is a lower triangular matrix defined by equation (13). For each vector entrée

$$\mathbf{M}_j = M_{d|X(0)}(-\exp(-y_j) | x) = u_{-\exp(-y_j)}(0, x) \quad (16)$$

a finite element solver is used to approximate the solution of the terminal value partial differential equation given by the Feynman-Kac formula. The solution to the minimization problem (15) can be obtained using a sequential least squares programming solver.

## RESULTS AND DISCUSSION

A comprising quantitative study of the impact of motion is not within the scope of this work. However, an investigation using the prerequisites shown in Figure 1 provides interesting qualitative results. The domain is circular and restricted by a border that terminates all paths that extends beyond it. A symmetric two-dimensional Gaussian concentration field is located at the centre of the domain, causing exposure of the uniformly distributed population. The probability distribution for the exposure of an individual depends on its starting position, with highest exposures in the middle of the domain and lowest exposures close to the domain border. The aggregated population injury,  $Q_r$ , as a whole is the main quantity of interest. Now, since both the domain and the concentration field are rotational symmetric with regards to the centre of the domain, the exposures for different positions depend only on the radial distance from origin.

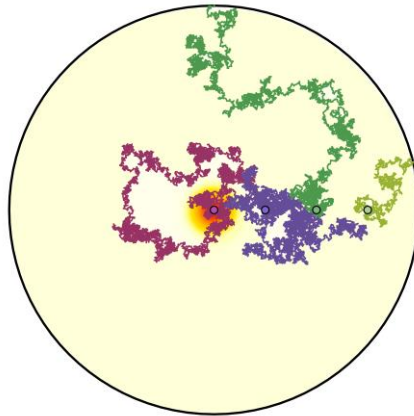


Figure 1. A circular domain with a centrally located Gaussian concentration field illustrated with a heat map. Four example paths are drawn together with their different starting positions, marked with circles. Paths are interrupted if they hit the border of the domain, as is the case for two of the paths in this example.

A probability distribution function can be found following the method described above. First, it is worth noticing that the calculated probability for injury may be considerably different using only the expectation value of  $\Theta$  in comparison to using the complete distribution thereof. For low exposures, the injury risk is underestimated when using the expectation value, while the opposite is true for high exposures. This finding is related to the so-called *impact region* shown in the left panel of Figure 2. The position and width of the impact region are determined by the substance-dependent probit values  $\alpha$  and  $\beta$ . Probability mass to the left of this region will give rise to negligible injury risk, while on the right side it will almost certainly cause injury. This is a strongly nonlinear relation which means that the distribution should be used, not only the expectation value.

As long as there are people left in the domain, the probability mass flows towards higher  $\Theta$ -values as time proceeds. The population injury,  $Q_r$ , increases as it enters the impact region with a maximum rate in the middle of the region.

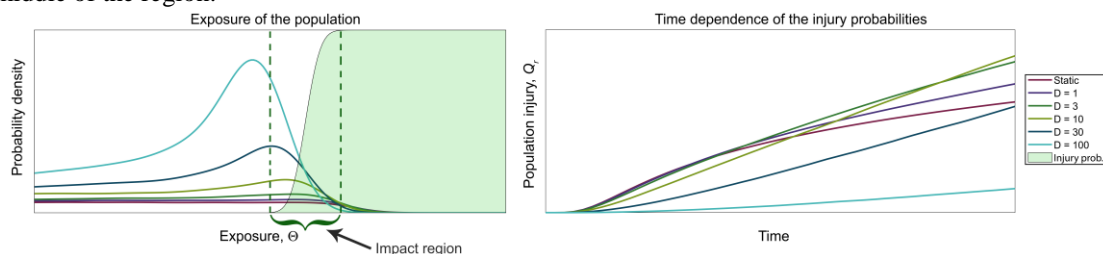


Figure 2. Left panel, the aggregated probability density distribution of  $\Theta$  for the entire population at the end time of the interval displayed in the right panel. Right panel, the injury outcome given the distribution of  $\Theta$  for different diffusion coefficients  $D$ . Note that “Static” actually corresponds to an almost static population; a very slow movement is actually used to obtain a non-discrete distribution. However, this slow movement does not interfere with the interpretation of the results.

As the right panel shows, slow movements (i.e., low diffusion coefficient  $D$ ) give rise to the earliest population injuries. The reason is that the persons initially exposed to high concentration remain there for a long time and therefore enters the impact region first. As time progresses things change, faster movements cause far more people to visit the region with high concentration and even though the probability for each person remains low,  $Q_r$  increases relatively fast.

It was found that the movement speed that maximize  $Q_r$  changes with time, illustrated in the right panel of Figure 2. This phenomenon might be non-intuitive at first, and it underlines the complexity of this field. Its direct implication is that there is no constant factor available to translate the population injury between different movement speeds. Instead, this finding motivates further and more thorough studies on the subject.

## REFERENCES

- Ashford, J., & Sowden, R. (1970). Multi-variate probit analysis. *Biometrics*, 535-546.
- Atherley, G. (1985). A critical review of time-weighted average as an index of exposure and dose, and of its key elements. *American Industrial Hygiene Association Journal*, 46(9), 481-487.
- Bliss, C. (1940). The relation between exposure time, concentration and toxicity in experiments on insecticides. *Annals of the Entomological Society of America*, 33(4), 721-766.
- Bliss, C. I. (1934). THE METHOD OF PROBITS. *Science*, 79(2037), 38-39. <https://doi.org/10.1126/science.79.2037.38>
- Bunce, N. J., & Remillard, R. B. (2003). Haber's Rule: the search for quantitative relationships in toxicology. *Human and Ecological Risk Assessment*, 9(4), 973-985.
- Czech, C., Platt, N., Urban, J., Bieringer, P., Bieberbach, G., Wyszogrodzki, A., & Weil, J. (2011). A comparison of hazard area predictions based on the ensemble-mean plume versus individual plume realizations using different toxic load models. 91st Annual American Meteorological Society Meeting, Seattle, Washington.
- Finney, D. J., & Tattersfield, F. (1952). *Probit analysis*. Cambridge University Press; Cambridge.
- Gardner, D., Miller, F., Blommer, E., & Coffin, D. (1979). Influence of exposure mode on the toxicity of NO<sub>2</sub>. *Environmental Health Perspectives*, 30, 23-29.
- Georgiadou, P. S., Papazoglou, I. A., Kiranoudis, C. T., & Markatos, N. C. (2007). Modeling emergency evacuation for major hazard industrial sites. *Reliability Engineering & System Safety*, 92(10), 1388-1402.
- Lovreglio, R., Ronchi, E., Maragkos, G., Beji, T., & Merci, B. (2016). A dynamic approach for the impact of a toxic gas dispersion hazard considering human behaviour and dispersion modelling. *Journal of Hazardous Materials*, 318, 758-771.
- Miller, F. J., Schlosser, P. M., & Janszen, D. B. (2000). Haber's rule: a special case in a family of curves relating concentration and duration of exposure to a fixed level of response for a given endpoint. *Toxicology*, 149(1), 21-34. [https://doi.org/10.1016/S0300-483X\(00\)00229-8](https://doi.org/10.1016/S0300-483X(00)00229-8)
- Milstein, G. N., & Tret'yakov, M. V. (2004). *Stochastic numerics for mathematical physics* (Vol. 456). Springer.
- Mocellin, P., & Vianello, C. (2022). A numerical study of effects of an industrial hazardous release on people egress. *Chemical Engineering Transactions*, 90, 445-450.
- Namboothiri, N. V., & Soman, A. (2018). Consequence assessment of anhydrous ammonia release using CFD-probit analysis. *Process safety progress*, 37(4), 525-534.
- Pontiggia, M., Derudi, M., Alba, M., Scaioni, M., & Rota, R. (2010). Hazardous gas releases in urban areas: Assessment of consequences through CFD modelling. *Journal of Hazardous Materials*, 176(1-3), 589-596.
- Rossberg, A. (2008). Laplace transforms of probability distributions and their inversions are easy on logarithmic scales. *Journal of applied probability*, 45(2), 531-541.
- Ten Berge, W., Zwart, A., & Appelman, L. (1986). Concentration—time mortality response relationship of irritant and systemically acting vapours and gases. *Journal of Hazardous Materials*, 13(3), 301-309.
- Wang, J., Yu, X., & Zong, R. (2020). A dynamic approach for evaluating the consequences of toxic gas dispersion in the chemical plants using CFD and evacuation modelling. *Journal of Loss Prevention in the Process Industries*, 65, 104156.